International Journal of Mass Spectrometry 285 (2009) 137–142

Contents lists available at ScienceDirect

International Journal of Mass Spectrometry

journal homepage: www.elsevier.com/locate/ijms

Nanostructured porous silicon by laser assisted electrochemical etching

J. Li[a], C. Lu[a,1], X.K. Hu[a], Xiujuan Yang[a], A.V. Loboda[b], R.H. Lipson[a,*]

[a] Department of Chemistry, University of Western Ontario, Chemistry Building, London, ON N6A 5B7, Canada
[b] MDS Analytical Technologies, 71 Four Valley Drive, Concord, ON L4K 2V8, Canada

ARTICLE INFO

Article history:
Received 6 April 2009
Received in revised form 20 May 2009
Accepted 21 May 2009
Available online 29 May 2009

Keywords:
Porous silicon
Laser assisted electrochemical etching
DIOS-MS

ABSTRACT

Nanostructured porous silicon (pSi) was fabricated by combining electrochemical etching with 355 nm laser processing. pSi prepared in this way proves to be an excellent substrate for desorption/ionization on silicon (DIOS) mass spectrometry (MS). Surfaces prepared by electrochemical etching and laser irradiation exhibit strong quantum confinement as evidenced by the observation of a red shift in the Si Raman band at ~520–500 cm^{-1}. The height of the nanostructured columns produced by electrochemical etching and laser processing is on the order of microns compared with tens of nanometers obtained without laser irradiation. The threshold for laser desorption and ionization of 12 mJ/cm^2 using the pSi substrates prepared in this work is lower than that obtained for conventional matrix assisted laser desorption ionization (MALDI)-MS using a standard matrix compound such as α-cyano-4-hydroxycinnamic acid (CHCA; 30 mJ/cm^2). Furthermore, the substrates prepared by etching and laser irradiation appear to resist laser damage better than those prepared by etching alone. These results enhance the capability of pSi for the detection of small molecular weight analytes by DIOS-MS.

1. Introduction

Matrix assisted laser desorption/ionization mass spectroscopy (MALDI-MS) has been extensively used to analyze large molecules such as synthetic polymers, proteins, carbohydrates and nucleic acids [1–5]. One of its limitations however, for the analysis of low molecular weight analytes is strong background interferences due to the organic matrix and/or fragments which can overlap the analyte ion signals in the mass spectra [6]. There has been considerable interest in developing matrix-free laser desorption/ionization (LDI) techniques to minimize this background matrix interference. Approaches include the use of porous silicon (pSi) [7], sol–gels [8] and carbon-based microstructures [9] as substrates. Among them, desorption ionization on silicon (DIOS) where bare pSi is used to desorb and ionize molecules instead of a matrix compound, has been widely employed to analyze a diverse range of samples including small drugs, explosives, polymers, and forensic compounds [10–13].

Several methods have been used to fabricate pSi [14–20]. One common approach is to electrochemically etch bulk Si wafers in dilute aqueous ethanol/hydrofluoric acid (HF) solutions [17–19]. The resultant structure however is mechanically fragile and unstable to oxidization. Alternatively, a pSi microcolumn array [14,20] can be created by exposing the Si substrate to a strong laser source. This methodology however tends not to be repeatable if the laser power is insufficient to melt the Si surface.

In this work, electrochemical etching and laser processing has been successfully combined. The resultant nanostructured pSi substrates exhibit excellent DIOS activity when used to analyze small molecules such as the polypeptide Dalargin.

2. Experimental

2.1. Preparation of nanostructured pSi

Nanostructured pSi was fabricated from n-type (arsenic-doped) silicon <1 0 0> wafers having a resistance <0.005 Ω cm. Each wafer was cleaned with a 5% HF/ethanol solution to remove the surface oxide layer, and then rinsed in deionized water, acetone, and methanol. Finally the wafer was dried in a gentle stream of N_2 gas. A schematic of the apparatus used to combine electrochemical etching and laser processing is shown in Fig. 1. The etching process was carried out at room temperature in a home-made Teflon electrochemical cell where the Si wafer served as the anode. The counter electrode was a platinum wire immersed into the electrolyte solution (HF, 48% by mass, Caledon Laboratories Ltd., Canada and ethanol; V_{HF}:$V_{Ethanol}$ = 1:1). The current density was maintained at 40 mA/cm^2. The top of the wafer was irradiated by the 4 ns pulses of a 355 nm frequency-tripled Nd:YAG laser (Spectra Physics, PRO-250) operating at a 20 Hz repetition rate, and with an inten-

* Corresponding author. Tel: +1 519 661 2111x86359; fax: +1 519 661 3022.
E-mail address: rlipson@uwo.ca (R.H. Lipson).
[1] Current address: Department of Chemistry, 80 St. George Street, University of Toronto, Toronto, ON M5S 3H6, Canada.

1387-3806/$ – see front matter © 2009 Elsevier B.V. All rights reserved.
doi:10.1016/j.ijms.2009.05.007

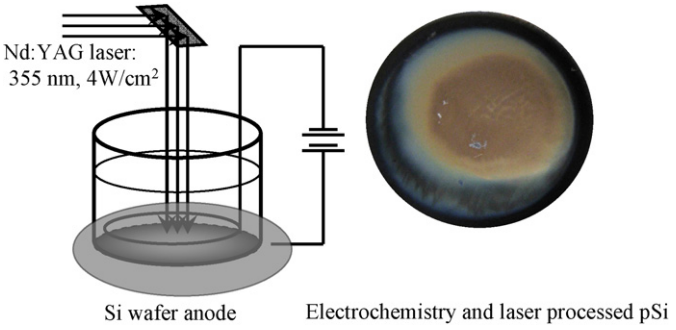

Fig. 1. Schematic illustration of the experimental arrangement for fabricating a pSi column array by laser assisted electrochemical etching.

sity of 4 W/cm^2. The best results were obtained when Si substrate was electrochemically treated for 5 min prior to laser irradiation for 15 min. The samples were stored in ethanol to avoid surface oxidation after rinsing with deionized water and methanol and carefully drying under a nitrogen gas flow.

2.2. DIOS-mass spectrometry

Mass spectra were acquired with a modified API-365 triple quadrupole mass spectrometer (MDS Analytical Technologies) that had a home-built MALDI interface installed. DIOS desorption was initiated by the 337 nm output of a pulsed N_2 laser (Laser Science Inc. Model VSL-337-ND-S, 20 Hz repetition rate) delivered to the Si sample via a 2-m UV fiber (Ocean Optics Inc., core diameter, 100 μm). An attenuator was used to control the laser fluence. Fluence values were calculated from the laser pulse energy measured at the output of the fiber, and the laser focal area was determined by the size of burn marks made on photographic paper. Each pSi substrate used in these experiments was attached with conductive double-side carbon tape to the insertion probe of a home-built MALDI front end chamber. The resultant ions were introduced into Q0 ion guide and their spectrum was recorded in Q1 scan mode. During the experiment, N_2 gas was introduced into the MALDI chamber to obtain pressure ~1 Torr near the target for ion cooling and collisional focusing.

Prednisolone (MW = 360.44 amu), Dalargin (MW = 725.4 amu), Bradykinin (MW = 1060.21 amu), and Adrenocorticotropic Hormone (ACTH) fragment 1–17 (MW = 2093.41 amu) were successfully detected using DIOS, but Dalargin ((HPLC grade, purity > 98%) was chosen as the primary analyte for presentation. 1 μM Darlagin solutions were prepared by dissolving the compound in acetonitrile-water $V_{CH_3CN} : V_{H_2O} = 70 : 30$ solution. The analyte solution was then spotted onto the nanostructured pSi surface with a micropipette and dried in air. MALDI mass spectra of Dalargin were recorded to compare with those obtained by DIOS using our pSi samples. Here, a solution of CHCA (100 mM) and Darlagin (1 μM) in a volume ratio of 60:1 was spotted onto the probe using a micropipette, and analyzed in the manner described above for DIOS-MS.

Scanning electron microscopy (SEM) images were obtained using a LEO-1540XB microscope. Raman spectra were acquired using a Confocal Raman instrument (Alpha SNOM, WITec, Germany) equipped with a 10 mW linearly polarized frequency-doubled Nd:YAG laser (λ = 532 nm, Verdi 5, Coherent Inc., Santa Barbara, CA). The beam focusing diameter was around 1 μm and the frequency resolution of the spectra is ±1 cm^{-1}.

3. Results and discussions

3.1. Characterization of Si surface structure

The morphology of pSi is known to be sensitive to the preparation conditions used, including the light intensity, the exposure

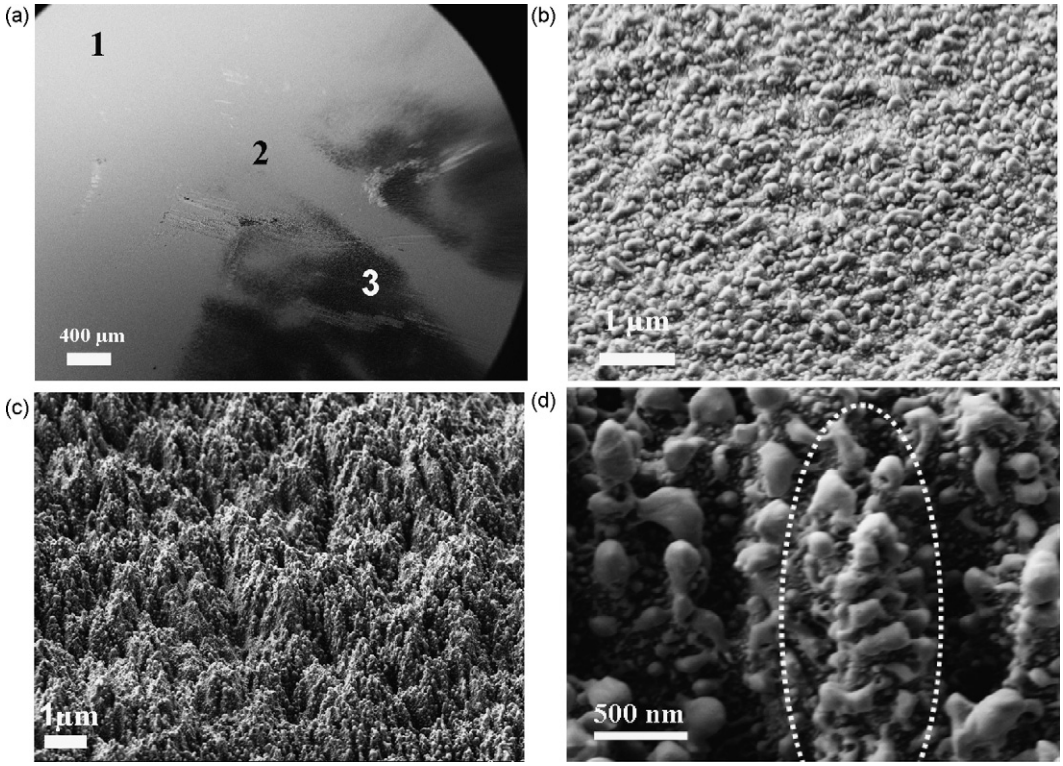

Fig. 2. (a) An overview SEM image of a Si sample after laser assisted electrochemical etching; 1 corresponds to a region without any processing, 2 to a region that was treated only by electrochemical etching, and 3 to a region treated by laser-assisted electrochemical etching; (b) a higher magnification SEM of Region 2; (c) a higher magnification SEM image of Region 3; and (d) an even higher magnification SEM image of Region 3. The dotted circle in (d) shows a nanoleaf formation.

time, the electrochemical etching current and even the etching chemical environment [14,19,21]. SEM images of the sample by irradiating the sample with 4 W/cm^2 of 355 nm laser intensity and electrochemically etching for 20 min are shown in Fig. 2. The Si chips were tilted 45° from normal during these measurements to show the depth of any surface features.

Fig. 2(a) presents an overview SEM image. No electrochemical etching or laser treatment was done in Region 1, while Regions 2 and 3 were electrochemically etched without and with direct laser exposure, respectively. Compared to Regions 1 and 2, Region 3 is darker grey and unreflective. Indeed, a shadow image of Pt electrode in Fig. 2(a) which blocked the laser beam is clearly visible between Regions 2 and 3. The low contrast between Regions 1 and 2 is a limitation of the detector at this resolution. The black color of processed silicon is indicative of a large absorption covering the UV to near-IR spectral range which is attributed to defect states in the band gap induced by structural defects formed during the etch treatment [20,22].

Region 1 under high magnification (not shown) shows a very smooth surface. In contrast Regions 2 and 3 are characterized by a rough surface morphology featuring many protrusions separated by tens to hundreds of nanometers. The difference between Regions 2 and 3 is that the etch depth of the former is ~tens of nanometers (Fig. 2(b)), while that of the latter is on the order of microns (Fig. 2(c). A closer inspection of nanostructured pSi shows that μm-long columns are spaced ~1 μm apart, and each column is covered by smaller nano-leaves with sizes in the range of tens to hundreds of nanometers (Fig. 2(d). These leaves can be removed by ultrasonic treatment in methanol.

Nanosecond laser pulse irradiation alone did not generate a profound change in the Si surface morphology which is opposite to that found using picosecond laser pulses [14]. This suggests that the peak intensity of the nanosecond pulses used in this work was insufficient to melt the Si substrate [20], a necessary requirement to generate pSi microcolumn arrays without electrochemical etching.

Nanostructured pSi formation appears to have been assisted by initial surface roughness generated by the electrochemical etching. It is well known that the large surface energy of porous/nanosilicon (200 mJ/cm^2 for porous silicon versus 0.1 mJ/cm^2 planar silicon) lowers the silicon melting temperature from 1410 °C to ~900 °C [23]. Thus the synergistic effects of electrochemical etching and laser irradiation can be understood as follows: the process of electrochemically etching effectively lowers the melting temperature of the surface which facilitates the deformation of the material by capillary waves generated upon laser irradiation. Small Si protrusions form upon laser exposure as Si vapour is redeposited onto the burgeoning columns which promotes their axial growth and deepens the troughs and canyons [14,24]. Nano-sized leaves on each column are formed by further electrochemical etching (Fig. 3).

As shown below the Si surfaces prepared by both electrochemical etching and laser processing have superior properties for DIOS compared to those made using other methods [14,21]. Furthermore, the greyish black surface in Region 3 proved to be robust to mechanical scratching, and there was no apparent damage after irradiating the sample with a laser fluence of 120 mJ/cm^2 for 1 h. On the other hand, the pSi formed by electrochemical etching only (Region 2) was found to be fragile to mechanical scratches and prolonged laser irradiation.

Raman spectroscopy is shown here to be an effective tool for probing the morphology changes induced by etching and irradiation. As shown in Fig. 4, the Raman spectra are measurably different in Regions A–C. In Region 1, the strong Raman optical phonon mode

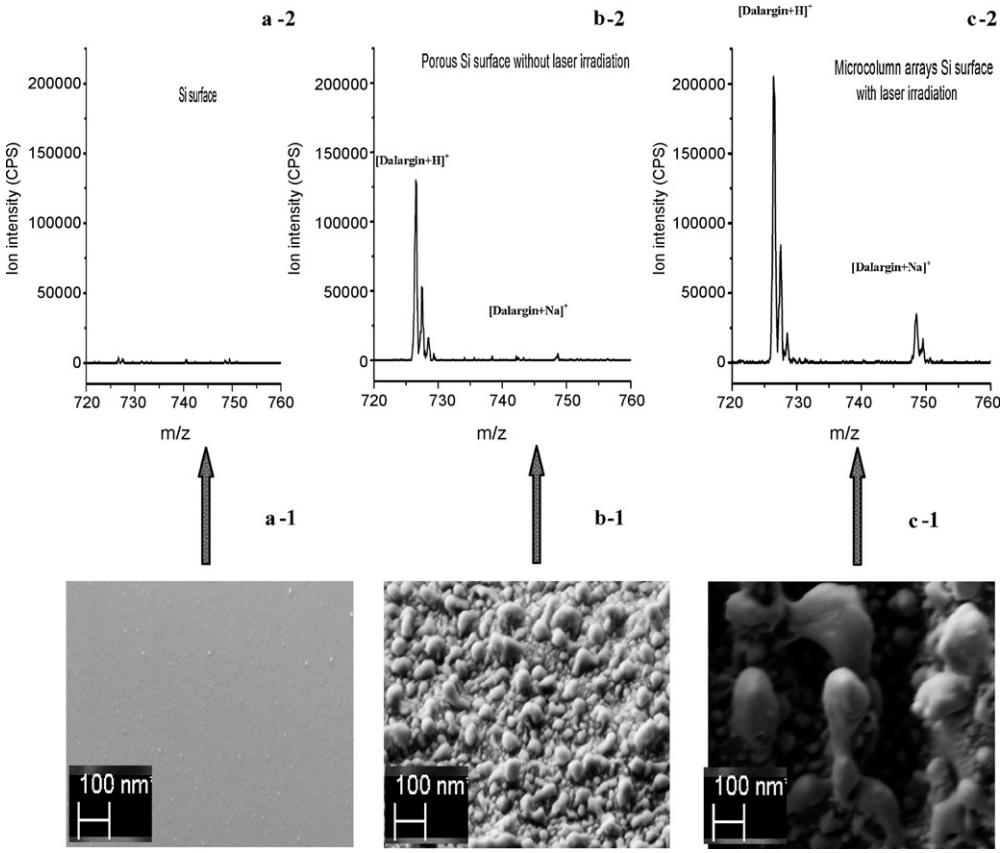

Fig. 3. (a-1), (b-1) and (c-1) are SEM images with magnification = 32 k× on an unetched spot, a spot that has been electrochemically etched, and a spot that has been electrochemically etched and laser irradiated, respectively; (a-2), (b-2) and (c-2) are DIOS-MS spectra of Dalargin obtained from the Si substrates shown in Regions 1–3 as denoted in Fig. 2.

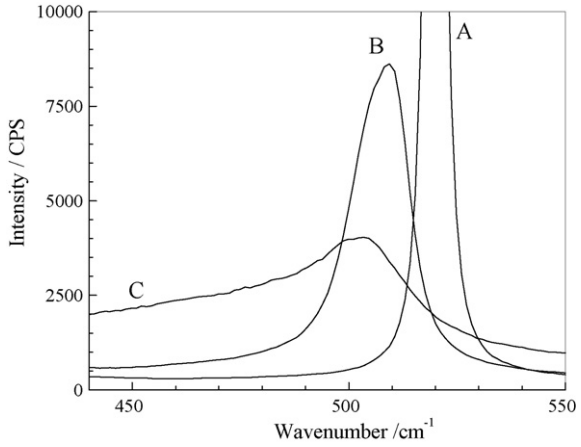

Fig. 4. Raman spectra of a Si chip. (A) A Si chip without any electrochemical etching or laser processing; (B) a Si chip treated by electrochemical etching for 20 min; and (C) a Si chip treated by laser assisted electrochemical etching.

of crystallized Si [25] is centered at 520 cm^{-1} and has a narrow full width at half maximum (FWHM) of 4.4 cm^{-1}. This spectral band red shifts to 509.4 cm^{-1} after electrochemical etching, and to 503.5 cm^{-1} after electrochemical etching with laser irradiation. Its peak intensity also decreases while its line shape broadens and becomes progressively more asymmetric. These changes are attributed to quantum size effects [25–27]. The magnitude of the frequency shift, peak width and the line shape asymmetry is inversely proportional to the size of the crystalline grain [25,26]. The results of this work suggest the combination of electrochemical etching and laser irradiation produces nano-size Si grains.

3.2. Deposition/ionization on Si

The ability of the nanostructured pSi surface to induce small molecule desorption and ionization was assessed by recording DIOS and MALDI spectra of the hexapeptide Dalargin whose dominant feature at m/z = 726.4 corresponds to the protonated [Darlagin+H]$^+$ signal. The Dalargin MALDI-MS spectrum shown in Fig. 5(a)) was recorded using CHCA as matrix and a N_2 laser fluence of 30 mJ/cm^2. The DIOS-mass spectrum using the same laser fluence can be found in Fig. 5(b). The analyte signal using CHCA is roughly 5 times stronger than the DIOS Dalargin signal but the DIOS spectrum has near-zero background noise. Conversely, the MALDI mass spectrum (Fig. 5(a)) exhibits many fragment and matrix-related peaks. A detection limit of 0.32 ± 0.04 pmol was obtained based on a standard curve made by plotting the signal-to-noise ratio of the DIOS-MS measurements against number of moles of Dalargin.

pSi surface morphology clearly appears to be the main factor leading to strong DIOS activity [28]. The correlation between morphology and DIOS signal intensity is attributed to several factors including the large substrate surface area and quantum confinement effects which manifest themselves through a large optical absorption and lower thermal conductivity [14]. An untreated Si surface (Region 1) did not produce any appreciable DIOS signals. Similar analyte ion signal strengths at 726.4 Da as those in Fig. 5(b) were found using pSi formed by electrochemical etching only, but only for short times. Fig. 6 shows the [Dalargin+H]$^+$ signals obtained as a function of time when using a N_2 laser fluence 30 mJ/cm^2 to irradiate a fixed location on the substrate. The signal obtained from a pSi substrate generated by just electrochemical etching disappears within 10 s. The surface was also noticeably damaged after laser irradiation, presumably due to the laser-induced surface melting and surface area rearrangement. On the other hand, the analyte signal obtained from pSi formed by electrochemical etching and

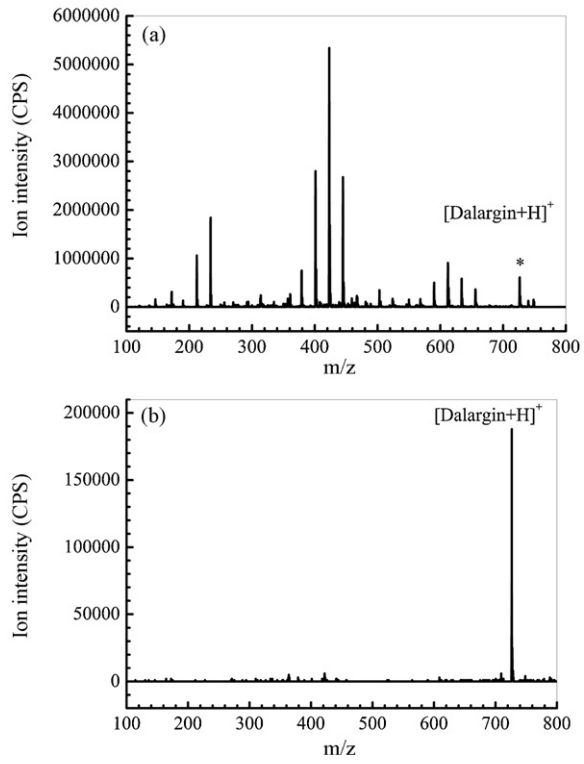

Fig. 5. (a) MALDI-MS spectra of Dalargin in CHCA matrix; (b) DIOS-MS spectrum of Dalargin from a pSi column array formed by electrochemical etching and ns laser processing.

laser processing dropped by only 50% after 60 s of irradiation. No noticeable damage to the substrate was found after prolonged exposure even the laser fluence was increased to 150 mJ/cm^2.

Laser-induced surface damage such as pore collapse and surface area loss, was previously reported by Northen et al. for electrochemically etched pSi samples [29]. The adsorbed analyte was expected to desorb quickly in Region 2 because the substrate here is composed of a very thin nano-porous layer. While the same surface melting process is expected to affect the nano-leaves formed on the columns of pSi in Region 3 the columns remain intact due to their relatively bigger sizes. The melted or ablated material then recrystallizes on the columns preserving the surface morphology. As a result, minimal structural changes were found for Region 3 after laser irradiation. Furthermore, the complex porous structure and large surface area act as a large analyte reservoir. For these reasons, the protonated Dalargin signal from Region 3 lasted much longer than that obtained from Region 2.

Fig. 7 shows for the first time the dependence of the DIOS signal of Dalargin (5 μL, 1 mM) on N_2 laser fluence. The laser fluence was varied between 6 mJ/cm^2 and 120 mJ/cm^2. Two findings are worth commenting on.

First, the laser fluence threshold of ~12 mJ/cm^2 required to desorb and ionize the Dalargin analyte from pSi is significantly lower than the value (~30 mJ/cm^2) reported for silicon microcolumn arrays produced by picosecond laser irradiation [8]. It is also lower than the threshold value found by MALDI experiments carried out in this work under the similar experimental conditions using CHCA (2 μL, 100 mM) as a matrix, which is also 30 mJ/cm^2.

Secondly, there are three regimes of DIOS activity that as shown in Fig. 7 correlate with laser fluence. In Regime I the onset of the protonated Dalargin DIOS signal occurs at ~12 mJ/cm^2 followed by approximately exponential signal growth between 12 mJ/cm^2 and 30 mJ/cm^2. The slope of the ln–ln plot of the data in this region is ~4. Typically, in a nonresonant nonlinear absorption process the

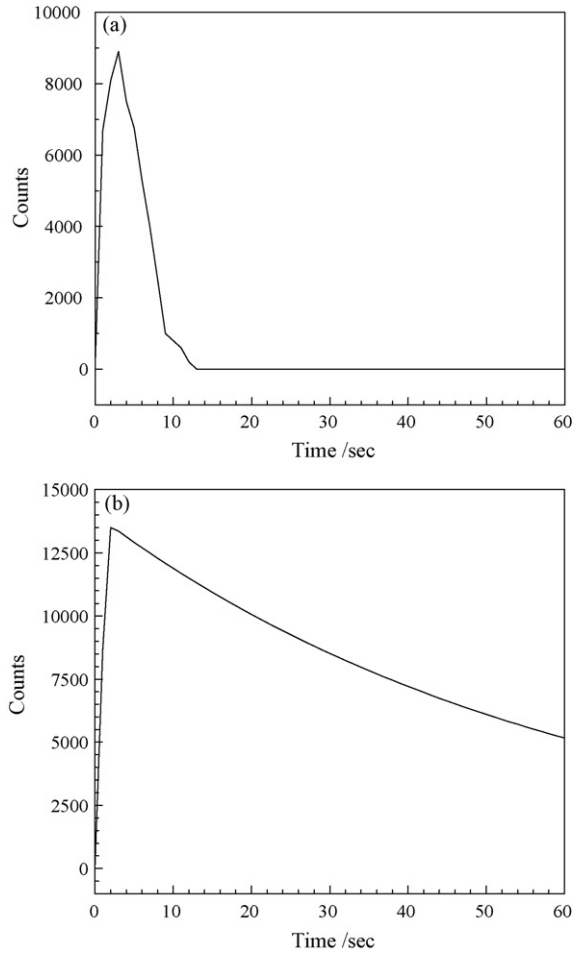

Fig. 6. The dependence of the protonated Dalargin analyte ion intensity on N_2 laser exposure time, generated by DIOS-MS at a fixed point on the substrate. (a) Using pSi formed by electrochemical etching alone; (b) a pSi column array formed by electrochemical etching and ns laser processing.

slope of a ln–ln plot of ion signal versus fluence indicates the number of photons involved [27]. Such an interpretation in this work is however unphysical given the low laser fluences used. Large slopes have also been observed for MALDI mass spectra irradiated by UV, visible and IR sources [30–33]. Conventional wisdom suggests that at low fluence ions are generated by molecular desorption and protonation. At higher fluences the ion signal saturates and declines (Regimes II and III), which is attributed to side reactions that lead to fragmentation and substrate surface deformation. Thus, it can be concluded that the initial step leading to primary ion formation using pSi is most likely thermal in nature [30].

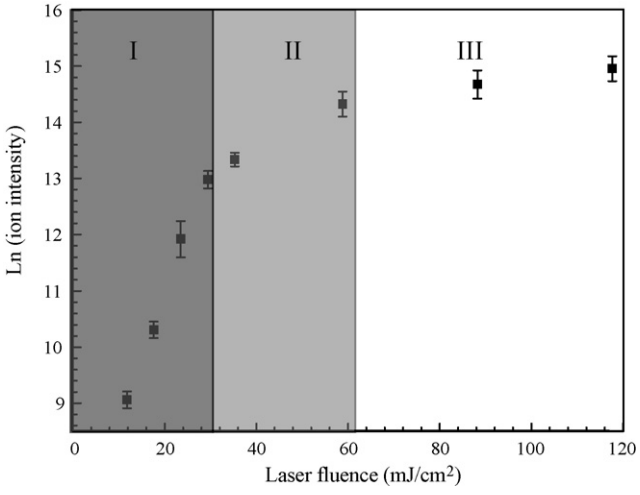

Fig. 7. A plot of the logarithm of the protonated Dalargin ion DIOS signal versus laser fluence using a pSi substrate fabricated by electrochemical etching and laser processing. The three different laser fluence-dependent regimes discussed in the text are labeled on the plot.

This thermal phenomenon and size effect further explain the large reduction in DIOS threshold. As noted above, the pSi is an array of modified columns covered with sub-micron or nano-sized leaves. The crystallites of Dalargin attached to the nano-leaves are most likely smaller than those found on a substrate without laser modification. Therefore, relatively lower laser fluences are needed for analyte desorption since smaller crystallites are known to be more volatile [34].

4. Conclusions

pSi formed by electrochemical etching and ns laser processing is characterized by a morphology of μm high Si columns covered by nano-leaves. Morphology of the new pSi substrate features large surface area that is relatively stable against UV laser damage. Combined electrochemical etching and laser processing of the surface allows ns laser pulses to be used for laser processing versus a more expensive ps or fs laser system. Finally our new method of creating pSi targets yields very reproducible results. Test runs using the analyte Dalargin found the laser fluence threshold for desorption and ionization to be ~12 mJ/cm^2, which is lower than that reported for pSi in the literature, and for conventional MALDI MS. The pSi substrates developed in this work show a promise to make DIOS-MS suitable for routine analysis of low molecular weight analytes.

Acknowledgements

This work was supported by the Natural Sciences and Engineering Research Council of Canada (NSERC), MDS Analytical Technology, the Ontario Centers of Excellence, and the University of Western Ontario.

References

[1] M. Karas, F. Hillenkamp, Anal. Chem. 60 (1988) 2299–2301.
[2] B. Stahl, A. Linos, M. Karas, F. Hillenkamp, M. Steup, Anal. Biochem. 246 (1997) 195–204.
[3] K. Tanaka, H. Waki, Y. Ido, S. Akita, Y. Yoshida, T. Yoshida, T. Matsuo, Rapid Commun. Mass Spectrom. 2 (1988) 151–153.
[4] K. Tang, N.I. Taranenko, S.L. Allman, L.Y. Chang, C.H. Chen, D.M. Lubman, Rapid Commun. Mass Spectrom. 8 (1994) 727–730.
[5] D. Lacey, X.K. Hu, A.V. Loboda, N.J. Mosey, R.H. Lipson, Int. J. Mass Spectrom. 261 (2007) 192–198.
[6] G. McCombie, R. Knochenmuss, Anal. Chem. 76 (2004) 4990–4997.
[7] J. Wei, J.M. Buriak, G. Siuzdak, Nature 399 (1999) 243–246.
[8] Y.-S. Lin, Y.-C. Chen, Anal. Chem. 74 (2002) 5793–5798.
[9] S.-f. Ren, Y.-l. Guo, Rapid Commun. Mass Spectrom. 19 (2005) 255–260.
[10] W.G. Lewis, Z. Shen, M.G. Finn, G. Siuzdak, Int. J. Mass Spectrom. 226 (2003) 107–116.
[11] J.J. Thomas, Z. Shen, R. Blackledge, G. Siuzdak, Anal. Chim. Acta 442 (2001) 183–190.
[12] Z. Shen, J.J. Thomas, C. Averbuj, K.M. Broo, M. Engelhard, J.E. Crowell, M.G. Finn, G. Siuzdak, Anal. Chem. 73 (2001) 612–619.
[13] S. Okuno, Y. Wada, R. Arakawa, Int. J. Mass Spectrom. 241 (2005) 43–48.
[14] Y. Chen, A. Vertes, Anal. Chem. 78 (2006) 5835–5844.
[15] G.-D. Anna, D. Jan, D. Wlodzimierz, K. Agnieszka, S. Jerzy, J. Vac. Sci. Technol. B 23 (2005) 819–823.
[16] J.D. Cuiffi, D.J. Hayes, S.J. Fonash, K.N. Brown, A.D. Jones, Anal. Chem. 73 (2001) 1292–1295.
[17] E.V. Astrova, T.N. Borovinskaya, A.V. Tkachenko, S. Balakrishnan, T.S. Perova, A. Rafferty, Y.K. Gun'ko, J. Micromech. Microeng. 14 (2004) 1022.
[18] S. Tuomikoski, K. Huikko, K. Grigoras, P. Ostman, R. Kostiainen, M. Baumann, J. Abian, T. Kotiaho, S. Franssila, Lab. A Chip 2 (2002) 247–253.
[19] V.V. Doan, R.M. Penner, M.J. Sailor, J. Phys. Chem. 97 (1993) 4505–4508.
[20] C.H. Crouch, J.E. Carey, J.M. Warrender, M.J. Aziz, E. Mazur, F.Y. Genin, Appl. Phys. Lett. 84 (2004) 1850–1852.

[21] J.W. Schultze, J. Porous Mater. 7 (2000) 11–16.
[22] C. Wu, C.H. Crouch, L. Zhao, J.E. Carey, R. Younkin, J.A. Levinson, E. Mazur, R.M. Farrell, P. Gothoskar, A. Karger, Appl. Phys. Lett. 78 (2001) 1850–1852.
[23] R. Herino, A. Perio, K. Barla, G. Bomchil, Mater. Lett. 2 (1984) 519–523.
[24] A.J. Pedraza, J.D. Fowlkes, D.H. Lowndes, Appl. Phys. Lett. 74 (1999) 2322–2324.
[25] B. Li, D. Yu, S.-L. Zhang, Phys. Rev. B 59 (1999) 1645.
[26] S. Zhifeng, P.L. Patrick, P.H. Irving, S.H. Gregg, T. Henryk, Appl. Phys. Lett. 60 (1992) 2086–2088.
[27] Z. Shu-Lin, D. Wei, Y. Yan, Q. Jiang, L. Bibo, L. Le-yu, Y. Kwok To, Y. Dapeng, Appl. Phys. Lett. 81 (2002) 4446–4448.
[28] S. Okuno, R. Arakawa, K. Okamoto, Y. Matsui, S. Seki, T. Kozawa, S. Tagawa, Y. Wada, Anal. Chem. 77 (2005) 5364–5369.
[29] T.R. Northen, H.-K. Woo, M.T. Northen, A. Nordström, W. Uritboonthail, K.L. Turner, G. Siuzdak, J. Am. Soc. Mass Spectrom. 18 (2007) 1945–1949.
[30] X.K. Hu, D. Lacey, J. Li, C. Yang, A.V. Loboda, R.H. Lipson, Int. J. Mass Spectrom. 278 (2008) 69–74.
[31] G. Westmacott, W. Ens, F. Hillenkamp, K. Dreisewerd, M. Schürenberg, Int. J. Mass Spectrom. 221 (2002) 67–81.
[32] W. Ens, Y. Mao, F. Mayer, K.G. Standing, Rapid Commun. Mass Spectrom. 5 (1991) 117–123.
[33] K. Dreisewerd, M. Schürenberg, M. Karas, F. Hillenkamp, Int. J. Mass Spectrom. Ion Processes 141 (1995) 127–148.
[34] M. Sadeghi, A. Vertes, Appl. Surf. Sci. 127-129 (1998) 226–234.